Water Filtration Machine with Monitoring System for Aquades Production and Founding an Optimal Pre-treatment Filter Ratio Before Reverse Osmosis Membrane

Ahmad Fauzan Adziimaa* & Muhamad Sultan Rasyiid

Department of Instrumentation Engineering, Institut Teknologi Sepuluh Nopember,
Jalan Raya ITS, Surabaya 60117, East Java, Indonesia
*E-mail: fauzan@its.ac.id

Abstract The increasing demand for distilled water (Aquades) in pharmaceutical and medical applications contrasts sharply with the limited quality of municipal water supplies and the high operating costs of commercial Aquades procurement. At the same time, many small-scale facilities still lack integrated systems capable of meeting the Indonesian Ministry of Health standard (Permenkes RI No. 32/2017). Existing research on reverse osmosis (RO) systems largely focuses on membrane or filtration performance, with limited attention to real-time water-quality monitoring and systematic optimization of pre-treatment filters. This study develops an integrated filtration and monitoring system designed to ensure regulatory compliance while optimizing the composition of pre-treatment materials. The system combines silica sand, activated carbon, and zeolite pre-filters with RO, supported by six analog sensors that continuously monitor pH, turbidity, and Total Dissolved Solids before and after filtration. Validation results show high sensor accuracy, with 99.77% for TDS, 98.10% for pH, and 99.97% for turbidity. Among six tested filter compositions, the 25% silica sand-25% activated carbon-50% zeolite configuration achieves the highest average filtration efficiency of 88.96%. These findings demonstrate that optimized pre-treatment combined with real-time monitoring can significantly improve RO performance and support cost-effective Aquades production for medical use.

Keywords *aquades production; pre-treatment filtration; real-time monitoring; reverse osmosis (RO); sensor validation; total dissolved solids (TDS); water purification system; water quality compliance.*

1 Introduction

The availability of high-quality water is a critical requirement in pharmaceutical and medical practices, as water quality directly influences equipment sterilization, analytical reliability, and patient safety [1][2]. The use of non-compliant water in laboratory and clinical environments may result in ineffective sterilization processes and increased risks of contamination and infection, thereby making water quality assurance not only an operational necessity but also a public health concern [3]. In many developing urban regions, including Indonesia, healthcare facilities rely heavily on municipal PDAM water supplies whose

Received October 6th, 2024, Revised 20 December 2025, Accepted for publication 23 December 2025.

quality may fluctuate temporally and spatially due to aging distribution infrastructure and variable treatment conditions [4].

Reverse osmosis technology has been widely adopted as an effective method for producing high purity water owing to its capability to remove dissolved ions, organic compounds, and microorganisms using semi permeable membranes [5, 6]. Numerous studies have demonstrated that RO systems can significantly improve water clarity and reduce Total Dissolved Solids, making them suitable for potable water production and laboratory scale applications [7, 8]. To enhance membrane performance and extend operational lifespan, various pretreatment strategies such as activated carbon adsorption, zeolite-based ion exchange, and sediment filtration have been introduced to mitigate fouling and reduce membrane loading [9-11].

Despite these technological advancements, most commercially available and laboratory scale RO systems operate without integrated real time monitoring of key physical water quality parameters, limiting the ability of users to verify output water compliance during continuous operation [12, 13]. Furthermore, existing studies often evaluate pretreatment media either individually or by adopting fixed material ratios without systematic optimization, resulting in inconsistent filtration performance across different water sources [14, 15]. Therefore, the optimization of pretreatment filter composition remains largely empirical, and its interaction with real time monitoring accuracy and overall system performance has not been sufficiently addressed.

To date, limited research has simultaneously integrated real time monitoring of multiple physical water quality parameters with systematic optimization of pretreatment filter composition within a single RO based water purification system intended for medical grade Aquades production. In particular, the relationship between pretreatment material ratios and overall filtration efficiency, when evaluated through validated sensor-based measurements before and after filtration, remains underexplored in existing literature [16, 17].

This study is based on the hypothesis that an optimized combination of silica sand, activated carbon, and zeolite in the pretreatment stage, when coupled with a calibrated multi sensor monitoring system, can significantly enhance filtration efficiency while ensuring consistent compliance with medical water quality standards [18, 19]. It is further assumed that systematic variation of material ratios will reveal a nonlinear performance trend, indicating the presence of an optimal composition rather than the dominance of a single filtration medium.

Accordingly, this research aims to develop an integrated water filtration and monitoring system that combines a multistage pretreatment filter with a reverse

osmosis membrane and real time measurement of pH, Total Dissolved Solids, and turbidity. In addition, this study explicitly seeks to identify the optimal pretreatment filter composition ratio that maximizes overall filtration efficiency while meeting the Indonesian Ministry of Health water quality standards [20].

The primary contribution of this work lies in the integration of sensor validated water quality monitoring with systematic pretreatment filter optimization in an RO based Aquades production system. Unlike previous studies that focus exclusively on filtration performance or sensor development, this research provides a data driven framework linking material composition, monitoring accuracy, and filtration efficiency within a single operational platform, thereby offering a practical and scalable solution for medical and pharmaceutical water treatment applications.

2 Related Work

Recent studies on water filtration systems have extensively explored the use of adsorption and ion exchange media to improve raw water quality prior to membrane based purification. A laboratory scale study investigated ammonia removal using activated carbon and zeolite as individual and hybrid filtration media, demonstrating that the combined filter exhibited higher efficiency in reducing ammonia, nitrite, and nitrate concentrations while maintaining stable pH levels compared to single media systems [21]. These findings confirm the synergistic effect of combining adsorption and ion exchange materials for enhancing filtration performance.

In the context of brackish water treatment, several studies have incorporated reverse osmosis systems supported by physical pretreatment stages and digital monitoring technologies. One study implemented locally sourced filter media integrated with an Internet of Things based monitoring system, reporting improvements in water clarity and odor removal; however, the treatment showed limited effectiveness in stabilizing pH and achieved only modest reductions in Total Dissolved Solids and electrical conductivity [22]. This highlights the importance of optimizing pretreatment design rather than relying solely on membrane filtration.

Membrane fouling remains a critical challenge in reverse osmosis systems, prompting investigations into fouling characterization and mitigation strategies. The Modified Fouling Index has been widely used to evaluate fouling potential in pretreated water, with studies reporting optimal operating pressures that maximize permeate flux and Total Dissolved Solids rejection while minimizing fouling rates [23]. Beyond fouling characterization, several studies emphasize the vulnerability of reverse osmosis membranes to excessive pressure and unstable

inflow conditions, which can lead to membrane damage and increased water wastage. To address these issues, control-based approaches have been proposed to regulate inflow rates and automatically terminate system operation when storage tanks reach predefined levels, thereby extending membrane lifespan and improving operational efficiency [24].

Accurate monitoring of water quality parameters is equally essential for evaluating filtration effectiveness. Previous research on sensor-based monitoring systems has focused on defining measurement error and accuracy through systematic sensor validation. Error is commonly defined as the deviation between sensor readings and reference values, while accuracy represents the degree of closeness between measured values and true values under specified conditions [25]. Building on these principles, recent studies have demonstrated the growing role of IoT-enabled architectures in real-time water management, where sensor feedback, automated control, and cloud-based data integration are employed to enhance irrigation efficiency and water consumption monitoring [26, 27].

In parallel, challenges related to membrane fouling, pressure sensitivity, and operational reliability have also been reported in membrane-based water treatment systems for critical applications, where inappropriate operating conditions can accelerate membrane degradation and shorten membrane lifespan [28]. Furthermore, pretreatment optimization strategies, such as the use of multi-media filtration for high-turbidity surface water, have been shown to effectively reduce particulate loading and fouling risk on downstream reverse osmosis membranes, highlighting the importance of integrated pretreatment and monitoring frameworks [29].

3 Methodology

In this section, we will discuss the methodology used in this research and describe the tools we use.

3.1 Properties of The Aquades Water Used

In the operation of pharmaceutical industries and medical practices in Surabaya, the Indonesian Ministry of Health Regulation No. 32 of 2017 is followed (Table 1), which outlines health quality standards for water used in hygiene and sanitation, including physical, biological, and chemical parameters that can be mandatory or additional. This research will highlight several key parameters to focus on, while excluding the numerous other parameters, to maintain clarity and direction

Table 1 Physical and Chemical Parameters in Water According to the Indonesian Minister of Health Regulation Number 32 of 2017, which are specifically discussed.

Parameters	Unit	Quality Standards (Maximum Rate)
Turbidity	NTU	≤ 25
Total Dissolved Solid	Mg/l	≤ 1000
Ph	Mg/l	6,5 – 8,5
Iron	Mg/l	≤ 0,2
Manganese	Mg/l	≤ 0,1

3.2 The Sediment is Combined in The Pre-treatment Filter

Typically, water undergoes a filtration process through various pre-filters before entering the Reverse Osmosis (RO) system is shown in Figure 1, and the choice of pre-filters is influenced by the water's Total Dissolved Solids (TDS) and its initial quality. Activated carbon filters are crucial for eliminating oxidative compounds such as chlorine, which can otherwise damage RO membranes, particularly Thin Film Composite (TFC) and Thin Film Membrane (TFM) types. Additionally, zeolite, a natural mineral known for its cation-exchange properties, effectively captures metal ions like iron (Fe), aluminum (Al), calcium (Ca), and manganese (Mn), thus reducing their concentrations in the water. Silica sand, composed of approximately 99.7% silicon dioxide (SiO_2), is particularly adept at filtering out physical impurities, including turbidity and odor, due to its fine granular structure. Sand & Miring (2023) recommend using a layer of silica sand with a thickness of 15 cm in the filter tube as an initial step in the filtration process to enhance the overall effectiveness of water purification systems.

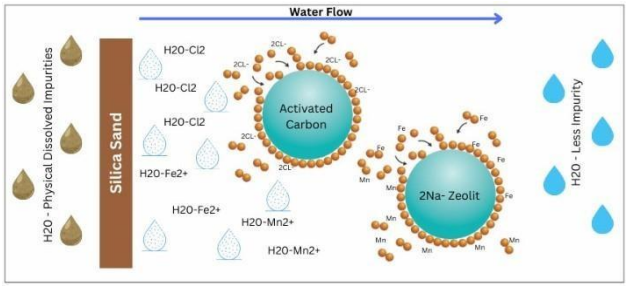

Figure 1 Sketch illustration of a simple chemical reaction.

3.3 Optimizing Pre-treatment Results using RO Membranes

To optimize the results of the pre-treatment filter media combination for producing distilled water, an RO membrane filter will be used as a constant variable, though it is not the main focus of this research. The 100 GPD reverse osmosis (RO) machine purifies tap water through multiple stages. First, sediment

filters remove various contaminants, while activated carbon absorbs chemicals like chlorine, zeolite captures iron and manganese, and silica sand filters dissolved particles. The crucial stage is the RO membrane, which has very small pores to filter out contaminants such as salts and bacteria, leaving only pure water.

3.4 Water Filtration Plant Design

Figure 2 shows the P&ID for the water filtration plant design. It starts with the feed water tank, which pumps water through three pre-treatment filters before it enters the reverse osmosis membrane. After reverse osmosis, the water passes through a post-carbon filter and then flows to the storage water tank. This research focuses on monitoring three parameters and comparing readings from the input and output of the filtration process.

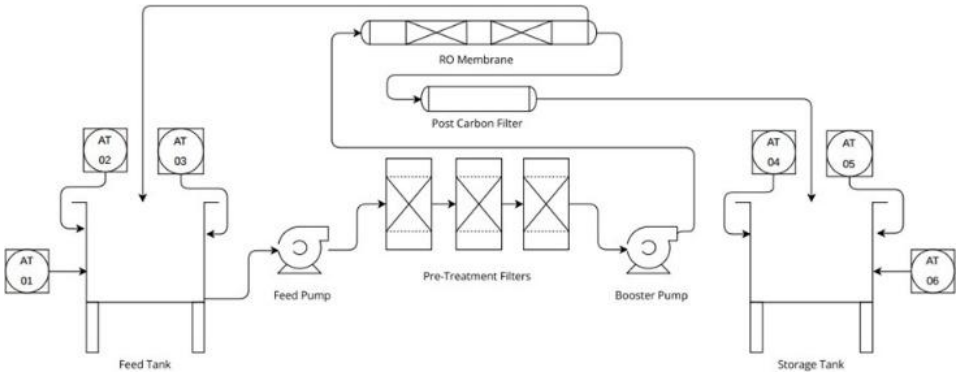

Figure 2 P&ID Water filtration plant.

3.5 Pre-Treatment Filter Volume Calculation

Before determining the material ratio to be tested, researchers must calculate the total volume of the filter cartridge to ensure even material distribution. This calculation is crucial for ensuring each filter section receives the correct amount of material, leading to consistent and reliable test results. Figure 3 illustrates the filter cartridge to help understand its structure and orientation, facilitating accurate volume calculation and material distribution.

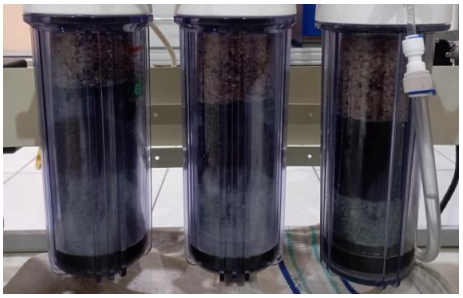

Figure 3 Filling Sediment in the Cartridge Filter for Pre-Treatment Filter.

After reviewing e-commerce listings, the researcher found dimensions listed as 6,5 cm of diameters and 19,5 cm tall. These dimensions can be used to calculate the volume of the cartridge, assuming it is a perfect cylinder, using geometric formulas by Eq. (1).

$$\begin{aligned} Volume &= \pi r^2 \; x \; t \\ &= 3.14 \; x \; 3{,}25^2 cm \; x \; 19{,}5 \; cm \\ &= 646{,}7 cm^3 \\ &= 0{,}6467 \; l = 0{,}6467 kg = 646 \; gr \end{aligned} \quad (1)$$

Monitoring System Architecture Figure 4 illustrates the comprehensive wiring diagram for the panel system responsible for monitoring critical water quality parameters including pH, turbidity, and Total Dissolved Solids (TDS). This diagram is a key reference for the author, detailing the intricate layout of the sensor circuits connected to a central microcontroller. The microcontroller interfaces with various signal conditioning components, which include a logic level controller designed to match voltage levels between different system parts, and a DC-DC step-down converter that reduces the input voltage from 24VDC to a stable 5VDC necessary for the operation of sensitive electronics. Additionally, the diagram includes the connections to the Human-Machine Interface (HMI) layer where real-time data is displayed for user interaction and monitoring. Furthermore, the wiring addresses provided below the diagram offer a detailed guide to the physical connections and signal paths within the system, ensuring accurate and reliable data transmission and control for effective water quality monitoring and management.

The design of the monitoring system for the water filtration plant is centered around three critical sensors that measure the input and output water quality at both the feed and storage tanks. Each sensor produces a 5VDC analog signal, which is essential for accurate water quality assessment. The pH sensor's output is routed through a logic level converter before reaching the ESP32 microcontroller; this converter adjusts the signal from 5V to 3.3V to match the operating voltage of the ESP32, thereby ensuring precise pH readings. In contrast,

the turbidity and TDS sensors provide signals that are inherently accurate and stable, eliminating the need for voltage conversion. After the initial signal conditioning, the analog signals are converted to digital format by the ESP32 for further processing. This digital data is then displayed on the LCD/HMI interface, allowing for real-time monitoring and user interaction.

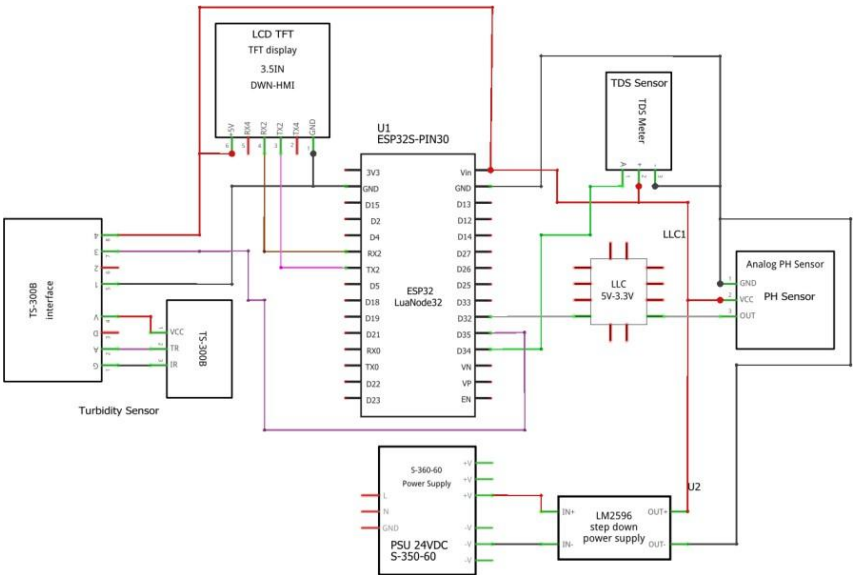

Figure 4 Wiring components of the monitoring system.

Figure 5 provides a detailed flow diagram illustrating the components associated with each sensor, along with their respective input and output variables, offering a clear depiction of how the system integrates and processes data from each sensor.

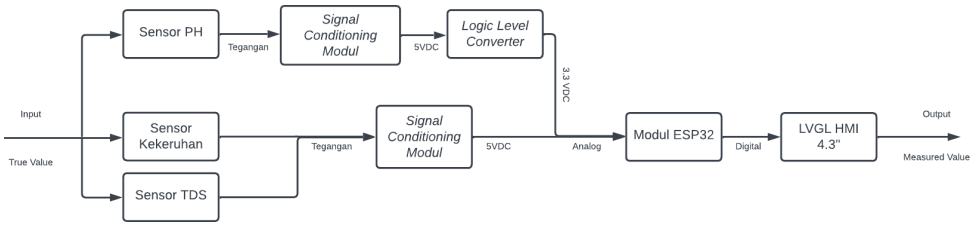

Figure 5 Measurement block diagram.

4 Construction of a Water Filtration Machine

This section will explain the manufacture of the water filtration machine that will be developed.

4.1 Designing of Water Filtration Machines

Figure 6 shows the prototype design of the water purification machine equipped with pre-treatment filters and a Reverse Osmosis membrane. This 3D design serves as a reference and depiction of the device, based on its function and layout. The machine uses an On-Off control system to operate an actuator in the form of a pump, which pushes the input water into three pre-treatment filter tanks, followed by passing through the Reverse Osmosis membrane. A panel box measuring 20x30x12 cm is also planned for use.

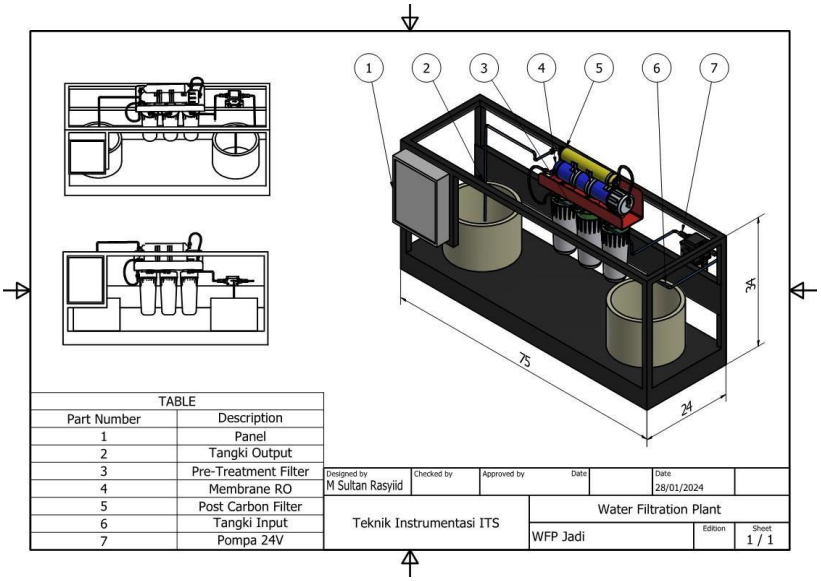

Figure 6 Prototype Water filtration plant.

4.2 Assembly of Water Filtration Machines

The hardware or mechanical construction of the process system is composed of several key components, each serving a distinct function to ensure efficient operation and maintenance. Firstly, the plant frame provides the structural support and foundation for the entire system. A custom-made water tank is designed to facilitate the installation of probes from various analyzer sensors, allowing for precise measurements and monitoring of water quality. Integrated with this tank is the reverse osmosis system, which is connected through crossover paths that facilitate the flow of water and maintain system efficiency. Additionally, the panel box serves as the central hub for electrical components, housing the controls and interfaces necessary for operation. Two sensor hubs are also included in the design, offering protection and organization for the electrical wiring and ensuring that the sensors are properly managed and shielded from

potential damage. This modular approach to hardware construction ensures that each component functions seamlessly within the overall system, contributing to the effective monitoring and filtration of water.

Figure 7 below shows the final form after the mechanical system design was completed. It resembles the initial design, featuring a main panel box with one HMI screen and one indicator light indicating the machine is active. Additionally, there is an RO machine with a capacity of 100 GPD used for laboratory-scale water purification.

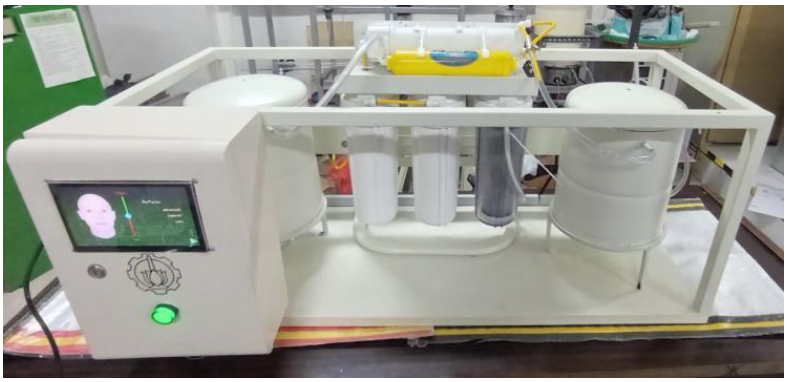

Figure 7 Prototype Water filtration plant.

Figure 8 below shows the interior of the water tank, which will have three sensors installed.

Figure 8 Documentation of Tank Conditions.

4.3 Design and Assembly for HMI

Figure 9 below shows the HMI (Human Machine Interface) design created by the author using the software provided by the hardware, namely Nextion Editor. The

initial design includes a single page with one main button labeled 'Start,' which, when pressed, initiates the plant operation according to the set process. The readings from six sensors, covering three parameters, are compared between the feed and storage tanks.

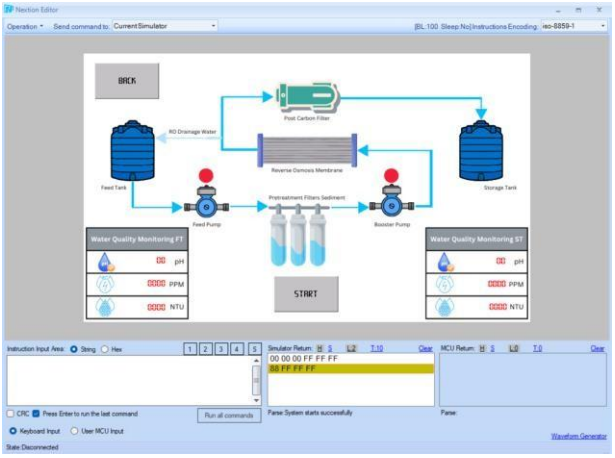

Figure 9 Flow Process View and Sensor Readings.

After editing the HMI, Figure 10 below documents the plant after the HMI design has been uploaded, facilitating the operation of the water filtration plant for the author.

Figure 10 HMI Documentation on the Plant.

4.4 Validation of Sensors in The Monitoring System

This section will be explaining the process of validation 6 sensors who read 3 parameters used to this machine.

4.4.1 Validation of TDS Sensors

Before conducting the research, the author needed to test the system. This involved validating the TDS sensor to ensure accurate readings. The author collected 30 validation data points, comparing sensor 1 (before) and sensor 2 (after) with a validator at two points: before and after. The solutions used were raw PDAM water and filtered water. After determining the average values, the data was processed to find the static characteristics of the Conductivity sensor integrated into the entire system, as shown in Table 2.

Table 2 Static Characteristics Table of TDS Sensor.

NO	Sensor 1 (Before) (PPM)	Validator (PPM)	Sensor 2 (After) (PPM)	Validator (PPM)
Average	417,40	419,00	34,16	35,00
Correction	1,60		0,84	
Error (%)	0,38		0,02	
Accuracy (%)	99,62		99,98	

The data can also be presented as a plot graph, making it easier to identify sensor characteristics, as shown in Figure 11(a) & (b) below.

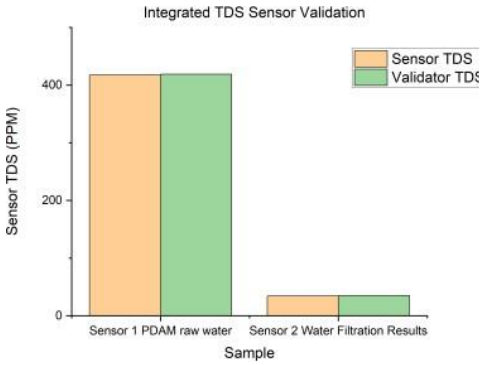

(a) Validation Graph of Two Conductivity Sensors.

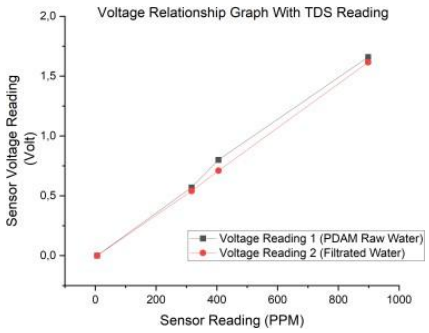

(b) Graph of Voltage and TDS Sensor Readings.

Figure 11 TDS Sensor characteristic graph.

During the validation process, a graph showing the relationship between voltage and sensor readings was obtained, as shown in Figure 11b. Both PDAM raw water and filtrated water exhibit strong linear voltage–TDS relationships, described by $V = 0.00199\ TDS + 0.040$ ($R^2 \approx 0.985$) and $V = 0.00194\ TDS + 0.020$ ($R^2 \approx 0.986$), respectively, indicating high linearity and comparable sensor sensitivity in both conditions. It demonstrates that higher voltage correlates directly with higher PPM sensor readings.

4.4.2 Validation of PH Sensors

Before conducting the research, the author validated the pH sensor to ensure accurate readings. The author collected 30 validation data points, comparing sensor readings before and after filtration with a validator at two points. The solutions used were raw PDAM water and filtered water. The average values were then used to determine the static characteristics of the pH sensor within the system, as shown in Table 3.

Table 3 Static characteristics table of PH sensor.

NO	sensor 1 (PH)	Validator (PH)	sensor 2 (PH)	Validator (PH)
Average	8,17	8,02	8,16	8,02
Correction	0,15		0,14	
Error (%)	1,91		1,81	
Accuracy (%)	98,09		98,19	

The data can also be presented as a plot graph, making it easier to identify sensor characteristics, as shown in Figure 12(a) & (b) below.

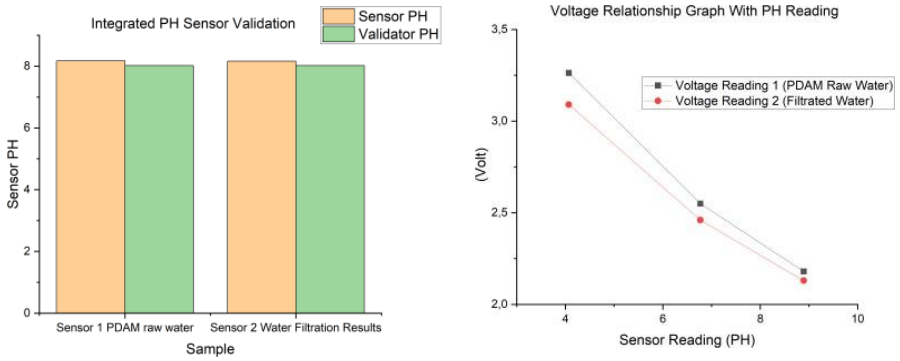

(a) Validation Graph of Two PH Sensors. **(b)** Graph of Voltage and PH Sensor Readings.

Figure 12 PH Sensor characteristic graph.

During the validation process, a graph depicting the relationship between voltage and sensor readings was obtained, as shown in Figure 12(b). Both PDAM raw water and filtrated water show strong negative linear relationships between voltage and pH, described by $V = -0.246\ pH + 4.21$ ($R^2 \approx 0.992$) and $V = -0.224\ pH + 3.97$ ($R^2 \approx 0.989$), respectively, indicating high linearity and consistent sensor response across both conditions. It indicates that as the voltage increases, the sensor readings are inversely proportional to the pH values.

4.4.3 Validation of Turbidity Sensors

Before commencing the research, the author performed a validation process on the TDS sensor to confirm its accuracy. This involved collecting thirty validation data points by comparing readings from sensor 1 (pre-validation) and sensor 2 (post-validation) against a standard reference validator. The comparison was conducted at two distinct stages: prior to and following the validation procedure. To streamline the process, only two types of solutions were used: raw PDAM water and filtered water. By averaging the collected values, the author was able to process the data to assess the static characteristics of the Conductivity sensor when it was integrated into the system.

The results of this analysis are detailed in Table 4, providing a comprehensive overview of the sensor's performance and reliability in the context of the overall system.

Table 4 Static Characteristics Table of Turbidity Sensor.

NO	Sensor 1 (Before) (NTU)	Validator (NTU)	Sensor 2 (After) (NTU)	Validator (NTU)
Average	42,23	42,34	1,45	1,43
Correction	0,11		0,02	
Error (%)	0,26		1.3	
Accuracy (%)	99,74		98.70	

The data can also be presented as a plot graph, making it easier to identify sensor characteristics, as shown in Figure 13(a) & (b) below.

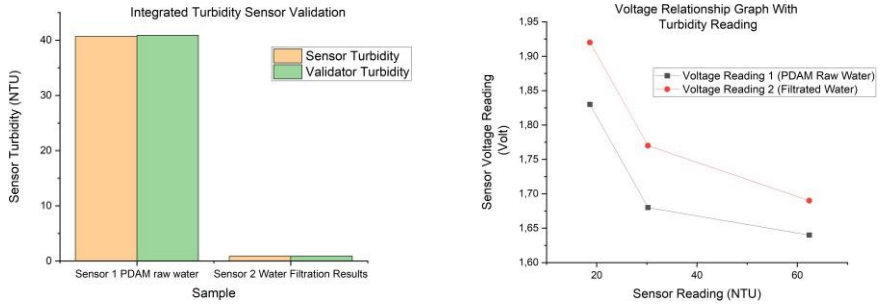

(a) Validation Graph of Two Turbidity Sensors.

(b) Graph of Voltage and Turbidity Sensor Readings.

Figure 13 Turbidity Sensor characteristic graph.

During the validation process, a graph was generated that depicts the relationship between voltage and sensor readings, as illustrated in Figure 13b. Both PDAM raw water and filtrated water exhibit weak-to-moderate negative linear relationships between voltage and turbidity, described by $V = -0.00396\ NTU + 1.86$ ($R^2 \approx 0.68$) and $V = -0.00496\ NTU + 1.97$ ($R^2 \approx 0.77$), respectively, indicating lower linearity compared to TDS and pH responses. This graph demonstrates that as the voltage increases, the sensor readings for turbidity (measured in NTU) exhibit an inversely proportional trend. In other words, higher voltage levels correspond to lower turbidity readings, indicating that the sensor's response to voltage changes affects its measurement of turbidity in a reverse manner. This inverse relationship highlights the sensitivity of the sensor to voltage variations and provides insights into its calibration and performance characteristics.

5 Comparison of 3 Sediment Ratios in Pre-Treatment Filter

In this section, experiments will be conducted on six combination compositions of sedimentary materials, including silica sand, activated carbon, and zeolite. The ratios have been determined based on the volume of the cartridge tube.

5.1 Composition 1

The first experiment uses Composition 1, as shown in Table 5 below, with a predetermined combination and sequence of sediments based on previous research. The author calculated the weight of the sediment to be filled into a 10-inch cartridge tube using the calculations explained in Subsection 3.5. The weight was then measured with a digital scale.

Table 5 Composition Used in Experiment 1.

	Cartridge 1	Cartridge 2	Cartridge 3
Si	60% (387,6 gr)	40% (258,4 gr)	20% (129,2 gr)
C	20% (129,2 gr)	30% (193,8 gr)	40% (258,4 gr)
Ze	20% (129,2 gr)	30% (193,8 gr)	40% (258,4 gr)

The results of this data collection are listed in Table 6 below, providing important information regarding the performance and response of the system or material being tested. This data will be further analyzed to evaluate and understand the characteristics and performance of the components under investigation.

Tabel 6 shows that the raw water has a pH of 8.18, TDS of 421.25 ppm, and turbidity of 43.57 NTU. After filtration with composition 1, the pH increased to 8.24, TDS decreased to 35.64 ppm, and turbidity dropped to 0.39 NTU. External laboratory analysis indicated a reduction in iron concentration from 0.11 mg/l to 0.043 mg/l, and manganese from 0.04 mg/l to 0.0093 mg/l, all below the threshold limits.

Table 6 Comparison of Physical and Chemical Parameters of Composition 1.

Parameters	Input Water	Filtered Water	RI Health Minister Regulation 2017 Standards	Parameter Reduction Percentage
pH	8,18	8,24	6,5 – 8,5	
TDS	421,25 PPM	38,64 PPM	≤ 1000 PPM	90,92%
Turbidity	43,57 NTU	0,39 NTU	≤ 2 5 NTU	99,10%
Iron	0,11 mg/L	0,043 mg/L	≤ 0,2 mg/L	60,90%
Manganese	0,04 mg/L	0,0093 mg/L	≤ 0,1 mg/L	76,75%
Average				81,9175%

5.2 Composition 2

The second experiment uses Composition 2, as shown in Table 7 below, with a predetermined combination and sequence of sediments based on previous research. The author calculated the weight of the sediment to be filled into a 10-inch cartridge tube using the calculations explained in Subsection 3.5. The weight was then measured with a digital scale.

Table 7 Composition Used in Experiment 2.

	Cartridge 1	Cartridge 2	Cartridge 3
Si	20% (129,2 gr)	30% (193,8 gr)	40% (258,4 gr)
C	60% (387,6 gr)	40% (258,4 gr)	20% (129,2 gr)
Ze	20% (129,2 gr)	30% (193,8 gr)	40% (258,4 gr)

The results of this data collection are listed in Table 8 below, providing important information regarding the performance and response of the system or material being tested. This data will be further analyzed to evaluate and understand the characteristics and performance of the components under investigation.

Tabel 8 shows that the raw water has a pH of 8.17, TDS of 415.90 ppm, and turbidity of 43.90 NTU, which are not within the desired Aquades standards. After filtration with composition 2, the pH decreased to 8.11, TDS reduced to 38.64 ppm, and turbidity dropped to 0.21 NTU. External laboratory analysis of the PDAM raw water and filtered water from composition 2 revealed that iron levels decreased from 0.11 mg/l to 0.043 mg/l and manganese from 0.04 mg/l to 0.0075 mg/l, both below the threshold limits.

Table 8 Comparison of Physical and Chemical Parameters of Composition 2.

Parameters	Input Water	Filtered Water	RI Health Minister Regulation 2017 Standards	Parameter Reduction Percentage
pH	8,17	8,11	6,5 – 8,5	
TDS	415,90 PPM	38,64 PPM	≤ 1000 PPM	90,70%
Turbidity	43,90 NTU	0,21 NTU	≤ 2 5 NTU	99,52%
Iron	0,11 mg/L	0,043 mg/L	≤ 0,2 mg/L	60,90%
Manganese	0,04 mg/L	0,0075 mg/L	≤ 0,1 mg/L	81,25%
Average				83,0925%

5.3 Composition 3

The third experiment employs Composition 3, detailed in Table 9 below, which utilizes a specific combination and sequence of sediments determined from prior research. The author calculated the required weight of sediment to be placed into a 10-inch cartridge tube using the calculations described in Subsection 3.1.2. Once the necessary weight was determined, it was measured using a digital scale to ensure precision. This process ensured that the sediment was accurately prepared according to the experimental parameters, providing a controlled basis for assessing the performance and effectiveness of the filtration system under the defined conditions.

Table 9 Composition Used in Experiment 3.

	Cartridge 1	Cartridge 2	Cartridge 3
Si	20% (129,2 gr)	30% (193,8 gr)	40% (258,4 gr)
C	20% (129,2 gr)	30% (193,8 gr)	40% (258,4 gr)
Ze	60% (387,6 gr)	40% (258,4 gr)	20% (129,2 gr)

The results from this data collection are detailed in Table 10 below, offering critical insights into the performance and response of the system or material under test. This table consolidates the data, which will be subjected to further analysis to assess and comprehend the characteristics and performance of the components being investigated. The subsequent analysis will help in evaluating the effectiveness of the system and understanding how each component behaves under various conditions, contributing to a thorough evaluation of the overall system's functionality and reliability.

Table 10 Comparison of Physical and Chemical Parameters of Composition 3.

Parameters	Input Water	Filtered Water	RI Health Minister Regulation 2017 Standards	Parameter Reduction Percentage
pH	8,17	8,21	6,5 – 8,5	
TDS	417,32 PPM	37,58 PPM	≤ 1000 PPM	90,99%
Turbidity	43,97 NTU	0,79 NTU	≤ 2 5 NTU	98,20%
Iron	0,11 mg/L	0,093 mg/L	≤ 0,2 mg/L	15,45%
Manganese	0,04 mg/L	0,0063 mg/L	≤ 0,1 mg/L	84,25%
Average				72,2225%

Table 10 shows that the raw water had a pH of 8.17, indicating it was within the normal neutral to slightly alkaline range, and TDS of 417.32 ppm, which is below the 1000 ppm standard but not yet considered aquades. Turbidity was 43.97 NTU, exceeding the aquades standard of 25 NTU. After filtration with composition 3, the pH increased slightly to 8.21, TDS decreased to 37.58 ppm, and turbidity reduced to 0.79 NTU. Analysis at the external PDAM Surya Sembada laboratory showed that iron levels decreased from 0.11 mg/l to 0.093 mg/l and manganese from 0.04 mg/l to 0.0063 mg/l, both below the threshold limits,.

5.4 Composition 4

The fourth experiment utilizes Composition 4, as detailed in Table 11 below, which involves a specific combination and sequence of sediments established through previous research.

Table 11 Composition Used in Experiment 4.

	Cartridge 1	Cartridge 2	Cartridge 3
Si	20% (129,2 gr)	20% (129,2 gr)	20% (129,2 gr)
C	20% (129,2 gr)	20% (129,2 gr)	20% (129,2 gr)
Ze	60% (387,6 gr)	60% (387,6 gr)	60% (387,6 gr)

To prepare for the experiment, the author calculated the weight of the sediment needed for filling a 10-inch cartridge tube, following the calculations outlined in

Subsection 3.1.2. This calculated weight was then precisely measured using a digital scale to ensure accuracy. This methodical approach ensures that the sediment is correctly prepared and accurately placed into the cartridge, providing a consistent basis for evaluating the performance and effectiveness of the filtration system during the experiment.

The results of this data collection are listed in Table 12 below, providing important information regarding the performance and response of the system or material being tested. This data will be further analyzed to evaluate and understand the characteristics and performance of the components under investigation.

Table 12 Comparison of Physical and Chemical Parameters of Composition 4.

Parameters	Input Water	Filtered Water	RI Health Minister Regulation 2017 Standards	Parameter Reduction Percentage
pH	8,16	8,14	6,5 – 8,5	
TDS	419,28 PPM	37,58 PPM	≤ 1000 PPM	91,03%
Turbidity	43,32 NTU	0,65 NTU	≤ 2 5 NTU	98,32%
Iron	0,11 mg/L	0,013 mg/L	≤ 0,2 mg/L	88,18%
Manganese	0,04 mg/L	0,0311 mg/L	≤ 0,1 mg/L	22,25%
Average				74,945%

Table 12 shows that the raw water had a pH of 8.16, within the normal neutral to slightly alkaline range, and TDS of 419.28 ppm, below the 1000 ppm standard but not considered aquades. Turbidity was 43.32 NTU, exceeding the aquades standard of 25 NTU. After filtration with composition 4, the pH slightly decreased to 8.14, TDS dropped to 37.58 ppm, and turbidity reduced to 0.65 NTU. External analysis at PDAM Surya Sembada laboratory showed that iron levels decreased from 0.11 mg/l to 0.013 mg/l and manganese from 0.04 mg/l to 0.0311 mg/l, both below the threshold limits.

5.5 Composition 5

The fifth experiment employs Composition 5, as detailed in Table 13 below, which consists of a specific combination and sequence of sediments based on earlier research. To prepare for the experiment, the author determined the weight of the sediment required for filling a 10-inch cartridge tube, utilizing the calculations provided in Subsection 3.5. After calculating the necessary weight, it was precisely measured using a digital scale to ensure accuracy. This meticulous preparation ensures that the sediment is accurately loaded into the cartridge, facilitating a consistent and reliable assessment of the filtration system's performance during the experiment.

Table 13 Composition Used in Experiment 5.

	Cartridge 1	Cartridge 2	Cartridge 3
Si	25% (161,5 gr)	25% (161,5 gr)	25% (161,5 gr)
C	25% (161,5 gr)	25% (161,5 gr)	25% (161,5 gr)
Ze	50% (323 gr)	50% (323 gr)	50% (323 gr)

The results from this data collection are presented in Table 14 below, offering critical insights into the performance and response of the system or material under examination. This table summarizes the collected data, which will undergo detailed analysis to assess and interpret the characteristics and effectiveness of the components being studied.

Table 14 Comparison of Physical and Chemical Parameters of Composition 5.

Parameters	Input Water	Filtered Water	RI Health Minister Regulation 2017 Standards	Parameter Reduction Percentage
pH	8,16	8,18	6,5 – 8,5	
TDS	420,65 PPM	36,88 PPM	≤ 1000 PPM	91,23%
Turbidity	44,47 NTU	0,36 NTU	≤ 2 5 NTU	99,19%
Iron	0,11 mg/L	0,013 mg/L	≤ 0,2 mg/L	88,18%
Manganese	0,04 mg/L	0,0091 mg/L	≤ 0,1 mg/L	77,25%
Average				88,9625%

Table 14 shows that the raw water had a pH of 8.16, within the normal neutral to slightly alkaline range, and a TDS of 420.65 ppm, below the 1000 ppm standard but not considered aquades. Turbidity was 44.47 NTU, above the 25 NTU aquades standard. After filtration with composition 5, the pH slightly increased to 8.18, TDS decreased to 36.88 ppm, and turbidity reduced to 0.36 NTU. External analysis at PDAM Surya Sembada laboratory revealed that iron levels dropped from 0.11 mg/l to 0.013 mg/l and manganese from 0.04 mg/l to 0.0091 mg/l, both below the threshold limits.

5.6 Composition 6

The sixth experiment utilizes Composition 6, outlined in Table 15 below, which includes a specific combination and sequence of sediments derived from prior research. For this experiment, the author calculated the required weight of the sediment to be filled into a 10-inch cartridge tube, following the calculation method described in Subsection 3.5. The calculated weight was then accurately measured using a digital scale to ensure precision. This careful measurement ensures that the sediment is correctly prepared and loaded into the cartridge,

providing a consistent and controlled basis for evaluating the filtration system's performance in the experiment.

Table 15 Composition Used in Experiment 6.

	Cartridge 1	Cartridge 2	Cartridge 3
Si	30% (193,8 gr)	30% (193,8 gr)	30% (193,8 gr)
C	30% (193,8 gr)	30% (193,8 gr)	30% (193,8 gr)
Ze	40% (258,4 gr)	40% (258,4 gr)	40% (258,4 gr)

The results from this data collection are summarized in Table 16 below, offering valuable insights into the performance and response of the system or material under examination. This table presents the data collected during the experiment, which will be subjected to further analysis to assess and interpret the characteristics and efficacy of the components being studied. The subsequent analysis will aim to understand how each component performs under the tested conditions, thereby contributing to a thorough evaluation of the system's overall functionality and reliability.

Table 16 shows that the raw water had a pH of 8.17, indicating it is within the normal neutral to slightly alkaline range but still below 8.5. The TDS was

416.27 ppm, below the 1000 ppm standard but not classified as aquades. Turbidity was 44.69 NTU, above the 25 NTU standard. After filtration with composition 6, the pH increased to 8.25, TDS decreased to 37.94 ppm, and turbidity reduced to 0.97 NTU. External analysis at PDAM Surya Sembada laboratory showed that iron levels dropped from 0.11 mg/l to 0.093 mg/l, and manganese from 0.04 mg/l to 0.0087 mg/l, both falling below the threshold limits.

Table 16 Comparison of Physical and Chemical Parameters of Composition 6.

Parameters	Input Water	Filtered Water	RI Health Minister Regulation 2017 Standards	Parameter Reduction Percentage
pH	8,17	8,25	6,5 – 8,5	
TDS	416,27 PPM	37,94 PPM	≤ 1000 PPM	90,88%
Turbidity	44,69 NTU	0,97 NTU	≤ 2 5 NTU	97,82%
Iron	0,11 mg/L	0,093 mg/L	≤ 0,2 mg/L	15,45%
Manganese	0,04 mg/L	0,0087 mg/L	≤ 0,1 mg/L	78,25%
Average				70,6%

6 Results and Discussion

Based on the data obtained from comparing all compositions of the material ratios of silica sand, activated carbon, and zeolite installed in the pre-treatment filter section before entering the reverse osmosis membrane, the average reduction in water parameter levels measured by the six sensors before and after the filtration process is as shown in Figure 14 below.

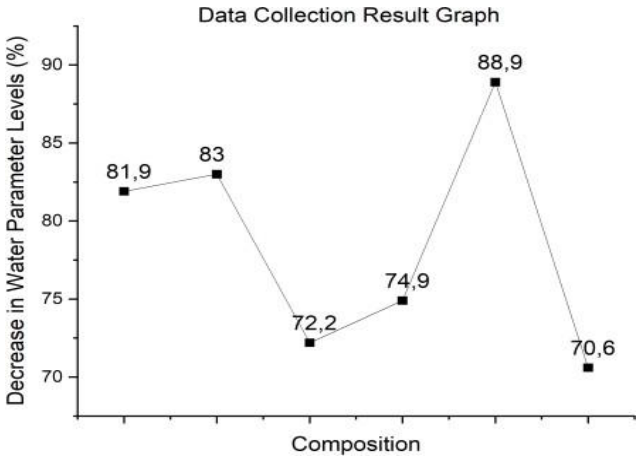

Figure 14 Graph of Parameter Reduction Rate.

7 Conclusion

Based on the validation test results, the TDS sensors' accuracy after assembly was 99.77% (TDS1) and 99.98% (TDS2). The pH sensors' accuracy was 98.10% (PH1) and 94.29% (PH2) after assembly. The turbidity sensors showed accuracy levels of 99.97% (Turbidity1) and 99.98% (Turbidity2). The pre- treatment filter composition tests revealed the following reduction rates: Composition 1 at 81.9%, Composition 2 at 83%, Composition 3 at 72.2%, Composition 4 at 74.9%, Composition 5 at 88.9%, and Composition 6 at 70.6%. Composition 5 was the most effective, achieving an average reduction rate of 88.9%, qualifying the filtered water as aquades. Among the six compositions, Composition 2 had the highest turbidity reduction at 99.52%, indicating its superior effectiveness in reducing turbidity levels.

Acknowledgement

The authors gratefully acknowledge financial support from the Institut Teknologi Sepuluh Nopember for this work, under project scheme of the Publication Writing and IPR Incentive Program (PPHKI) 2025.

References

[1] Yang, Z., Zhou, Y., Feng, Z., Rui, X., Zhang, T. & Zhang, Z., *A Review on Reverse Osmosis and Nanofiltration Membranes for Water Purification*, Polymers, **11**(8), 2019. DOI: 10.3390/polym11081254.

[2] Pezeshki, H., Hashemi, M. & Rajabi, S., *Removal of Arsenic from Drinking Water by Nanofiltration and Reverse Osmosis Techniques*, Heliyon, **9**(3), e14246, 2023. DOI: 10.1016/j.heliyon.2023.e14246.

[3] Maselela, J.L., Mokgobu, M.I. & Mudau, L.S., *A Regulatory Framework for Bottled Water Quality Monitoring*, Heliyon, **10**(10), e31543, 2024. DOI: 10.1016/j.heliyon.2024.e31543.

[4] González, P.S., Stehr, A. & Barra, R.O., *Assessment of Water Quality Trends Using Aggregated Indices*, Ecological Indicators, **166**, 112373, 2024. DOI: 10.1016/j.ecolind.2024.112373.

[5] Cornelissen, E.R., Harmsen, D.J.H. & Blankert, B., *Effect of Minimal Pretreatment on Reverse Osmosis Performance*, Desalination, **509**, 115056, 2021. DOI: 10.1016/j.desal.2021.115056.

[6] Parsa, S.M., *Mega Scale Desalination Efficacy during COVID-19*, Journal of Hazardous Materials Advances, **9**, 100217, 2023. DOI: 10.1016/j.hazadv.2023.100217.

[7] Mohammed, H.A., Sachit, D.E. & Al Furaiji, M.H., *Treatment of Power Plant Wastewater Using RO*, Desalination and Water Treatment, **283**, 29192, 2023. DOI: 10.5004/dwt.2023.29192.

[8] Hermawan, S., Pranata, F.J. & Limantara, I.R., *Brackish Water Treatment Using Local Materials*, Civil Engineering Dimension, **25**(1), pp. 53-75, 2023. DOI: 10.9744/ced.25.1.53-66.

[9] Daulay, A.H. & Manalu, K., *Activated Carbon and Zeolite Combination for Water Treatment*, JISTech, 4(2), 2019. DOI: N/A.

[10] Yu, L.J., Rengasamy, K. & Lim, K.Y., *Comparison of Activated Carbon and Zeolite Efficiency*, Journal of Environmental Chemical Engineering, **7**(4), 103223, 2019. DOI: 10.1016/j.jece.2019.103223.

[11] Cala, A., Maturana Córdoba, A. & Soto Verjel, J., *Pretreatment Influence on Reverse Osmosis Performance*, Renewable and Sustainable Energy Reviews, **188**, pp.1-14, 2023. DOI: 10.1016/j.rser.2023.113874.

[12] Almawgani, A.H.M., *Smart Monitoring System of Najran Dam*, International Journal of Electrical and Computer Engineering, **10**(4), pp. 3999~4007, 2020. DOI: 10.11591/ijece.v10i4.pp4045-4054.

[13] Mohd Jais, N.A. & Abdullah, A.F., *Improved Accuracy in IoT-Based Water Quality Monitoring,* Heliyon, **10**(8), e29022, 2024. DOI: 10.1016/j.heliyon.2024.e29022.

[14] Bidari, M., Putri, M.A. & Nasir, S., *Effect of Activated Carbon on RO Membrane Fouling*, Jurnal Teknik Kimia, **28**(3), pp. 100-106, 2022. DOI: N/A.

[15] Abushaban, A., Salinas Rodriguez, S.G. & Kennedy, M.D., *Pretreatment and Seawater RO Performance Assessment,* Desalination, **467**, pp 210-218, 2019. DOI: 10.1016/j.desal.2019.06.006.
[16] Altmann, T., Rousseva, A. & Vrouwenvelder, J., *Effectiveness of Ceramic Ultrafiltration Pretreatment*, Desalination, **564**, pp 1-14, 2023. DOI: 10.1016/j.desal.2023.116703.
[17] Minier-Matar, J. & AlShamari, E., *Evaluation of RO Membrane Fouling in Industrial Wastewater*, Desalination, **572**, pp 1-15, 2024. DOI: 10.1016/j.desal.2024.116942.
[18] Sand, S. & Miring, T., *Design of Filtration Systems Using Silica Sand and Activated Carbon*, Applied Environmental Engineering, 2023. DOI: N/A.
[19] Jebur, M. & Chiao, Y.H*., Electrocoagulation as RO Pretreatment*, Water Resources and Industry, **31**, 100243, 2024. DOI: 10.1016/j.wri.2024. 100243.
[20] Indonesian Ministry of Health, Regulation No. 32 of 2017 on Water Quality Standards, 2017. DOI: N/A.
[21] Yu, L.J., Rengasamy, K., Lim, K.Y., Tan, L.S., Tarawneh, M., Zulkoffli, Z.B. & Se Yong, E.N., *Comparison of Activated Carbon and Zeolites Filtering Efficiency in Freshwater*, Journal of Environmental Chemical Engineering, **7**(4), 103223, 2019. DOI: 10.1016/j.jece.2019.103223.
[22] Hermawan, S., Pranata, F.J., Limantara, I.R., Steven, D., Fernaldi, J. & Prajogo, J.E., *A Practical Implementation of Brackish Water Treatment with Local Material Aided by IoT Technology*, Civil Engineering Dimension, **25**(1), pp. 53-66, 2023. DOI: 10.9744/ced.25.1.53-66.
[23] Abushaban, A., Salinas Rodriguez, S.G., Dhakal, N., Schippers, J.C. & Kennedy, M.D., *Assessing Pretreatment and Seawater Reverse Osmosis Performance Using Modified Fouling Index*, Desalination, **467**, pp. 210-218, 2019. DOI: 10.1016/j.desal.2019.06.006.
[24] Cornelissen, E.R., Harmsen, D.J.H., Blankert, B., Wessels, L.P. & van der Meer, W.G.J., *Effect of Minimal Pretreatment on Reverse Osmosis Using Surface Water as a Source*, Desalination, **509**, 115056, 2021. DOI: 10.1016/j.desal.2021.115056.
[25] Mohd Jais, N.A., Abdullah, A.F., Mohd Kassim, M.S. & Abd Karim, M.M., *Improved Accuracy in IoT-Based Water Quality Monitoring Using Low-Cost Sensors*, Heliyon, **10**(8), e29022, 2024. DOI: 10.1016/j.heliyon.2024.e29022.
[26] Gokul, V., Sivaramakrishna, R.V., Vignesh, P., Ramesh, P., Bino, J. & Bhuvaneswari, P.T.V., *ISIS: IoT Enabled Smart Irrigation System*, Advances in Emerging Technologies and Computing Innovations, Springer, Cham, 2025. DOI: 10.1007/978-3-031-92854-3_2.
[27] Shabana Parveen, M., Lakshana, S.I., Saranya, P., Avanthika, S., Ramesh, P. & Bino, J., *SI-SWCS: IoT Enabled Smart Water Consumption System with Cloud Integration*, Advances in Emerging Technologies and

Computing Innovations, Springer, Cham, 2025. DOI: 10.1007/978-3-031-92854-3_6.

[28] Alzahrani, B. & Mohammad, A.W., *Challenges in Membrane-Based Water Treatment Systems for Healthcare Applications*, Desalination, **351**, pp. 6-17, 2014. DOI: 10.1016/j.desal.2014.07.012.

[29] Gharaibeh, S., Al-Ruz, F., Al-Abazi, R., Al-Sultan, K., *Optimization of Multi-Media Filter Composition for High-Turbidity Surface Water*, Environmental Technology, **40**(23), pp. 3067-3078, 2019. DOI: 10.1080/09593330.2018.1460932.